National Laboratory, Report ANL/ES-CEN-1001 (1969).
Lachapelle, D. G., J. S. Bowen, and R. D. Stern, "Overview of Environmental Protection Agency's NO_x Control Technology for Stationary Combustion Sources," paper presented at 67th Annual Meeting, AIChE, Washington, D.C. (Dec., 1974).
Martin, G. B., and E. E. Berkau, "Evaluation of Various Combustion Modifications Techniques for Control of Thermal and Fuel Related Nitrogen Oxides Emissions," paper presented at 14th Symposium (International) on Combustion, University Park, Pa. (1972).
———, "An Investigation of the Formation of Various Fuel Compounds to Nitrogen Oxides in Oil Combustion," *AIChE Symposium Ser. No. 68*, 45-54 (1972).
McCann, C. R., J. M. Henry, J. J. Demeter, and D. Bienstock, "Control of NO_x Emissions in Pulverized Coal Combustion," U.S. Bureau of Mines, Pittsburgh Energy Center, Pa. U.S. Bureau of Mines Report of Investigations (1974).
McCann, C. R., J. J. Demeter, A. A. Orning, and D. Bienstock, "Combustion of Pulverized Char," paper presented at Am. Chem. Soc. Meeting, Washington, D.C. (1971).
Mulcahy, M. F. R., and I. W. Smith, "Kinetics of Combustion of Pulverized Fuel: A Review of Theory and Experiment," *Rev. Pure Appl. Chem.*, **19**, 81 (1969).
Myerson, A. L., "The Reduction of Nitric Oxide in Simulated Combustion Effluents by Hydrocarbon-Oxygen Mixtures," *Fifteenth Symposium (International) on Combustion*, p. 1085, The Combustion Institute, Pittsburgh, Pa. (1975).
Pereira, F. J., J. M. Beér, B. Gibbs, and A. B. Hedley, "NO_x Emissions from Fluidized Bed Coal Combustors," *Fifteenth (International) Symposium on Combustion*, p. 1149, The Combustion Institute, Pittsburgh, Pa. (1975).
Pershing, D. W., G. B. Martin, and E. E. Berkau, "Influence of Design Variables on the Production of Thermal and Fuel NO from Residual Oil and Coal Combustion," AIChE Symposium Series No. 148, **71**, 19 (1975).
Petersen, E. E., *Chemical Reaction Analysis*, Prentice Hall, Englewood Cliffs, N. J. (1965).
Sarofim, A. G., G. C. Williams, M. Modell, and S. M. Slater, "Conversion of Fuel Nitrogen to Nitric Oxide in Premixed and Diffusion Flames," AIChE Symposium Series No. 148, **71**, 51 (1975).
Schulze, O. E., "Formation of Pollutants During Char Combustion," M.S. thesis, Univ. Ariz., Tucson (Aug., 1974).
Smith, I. W., "The Kinetics of Combustion of Pulverized Semi-Anthracite in the Temperature Range 1400-2200°K," *Comb. Flame*, **17**, 421 (1971).
———, and R. J. Tyler, "Internal Burning of Pulverized Semi-Anthracite: The Relation Between Particle Structure and Reactivity," *Fuel*, **51**, 312 (1972).
Sternling, C. V., and J. O. L. Wendt, "Kinetic Mechanisms Governing the Fate of Chemically Bound Sulfur and Nitrogen in Combustion," NTIS Report No. PB-230895, U.S. Department of Commerce, Springfield, Va. (1972).
———, "On the Oxidation of Fuel Nitrogen in a Diffusion Flame," *AIChE J.*, **20**, 81 (1974).
Wendt, J. O. L., and C. V. Sternling, "Effect of Ammonia in Gaseous Fuels on NO_x Emissions," *J. Air Poll. Control Assoc.*, **24**, 1055 (1974).
———, and M. A. Matovich, "Reduction of Sulfur Trioxide and Nitrogen Oxides by Secondary Fuel Injection," *Fourteenth Symposium (International) on Combustion*, p. 897, The Combustion Institute, Pittsburgh, Pa. (1973).

Manuscript received February 25, 1975; revision received October 15, and accepted October 17, 1975.

Secondary Nucleation of Two Fast Growth Systems in a Mixed Suspension Crystallizer: Magnesium Sulfate and Citric Acid Water Systems

Secondary nucleation of magnesium sulfate and citric acid was studied in a seeded back mixed crystallizer. The MSMPR type of exponential population density distribution was obtained above 8 μm size in quasi steady state operation. Growth rates were satisfactorily correlated with supersaturation. Nucleation rates correlated with supersaturation and slurry properties. Agitation level (RPM) did not have any significant effect on the nucleation rates, presumably implying surface regeneration limited nucleation.

SUBHAS K. SIKDAR
and
ALAN D. RANDOLPH

Department of Chemical Engineering
University of Arizona
Tucson, Arizona 85721

SCOPE

Mixed suspension crystallizers of the kind used in this study proved to be an excellent tool for the determination of kinetics of fast growth systems such as magnesium sulfate heptahydrate and citric acid monohydrate. Continuous on-line measurement of the fines distribution created by secondary nucleation with a short average fluid retention time and with the parent seed crystals totally retained in the crystallizer is a desirable feature of this technique. In addition to measuring effective growth and nucleation kinetics, the technique furnishes insight into the fundamental mechanisms of secondary nucleation. The mini-crystallizer of this study operates as a realistic MSMPR crystallizer, yet offers distinct advantages over conventional MSMPR techniques. For example, the supersaturation and the retention time can be independently varied, while the time scale of the entire experiment is shortened considerably. The effect of the different moments of macrosized crystals can be independently measured. The kinetic correlations obtained in this study could be gainfully utilized in the design of crystallizers. Continuous fines distribution measurement was possible by the use of a multichannel Coulter Counter.

Correspondence concerning this paper should be addressed to A. D. Randolph. S. K. Sikdar is with Garrett Research and Development Company, Inc., La Verne, California 91750.

CONCLUSIONS AND SIGNIFICANCE

Three conclusions are made in this study:

1. The size-independent growth rate (for sizes >8 μm) of magnesium sulfate reported by previous investigators has been verified. A similar conclusion was made for the growth rate of citric acid monohydrate crystals as well.

2. Design oriented kinetics were obtained from a system where both nucleation and growth of crystals were occurring. The correlations that are presented also furnish information as to the mechanisms of the nucleation process. Thus, the absence of an RPM function in both the growth rate and nucleation rate correlations indicates that growth rates are controlled by the particle integration step, and that nucleation rates are surface regeneration controlled.

3. Below 8 μm size, more nuclei were counted than could be accounted for by the MSMPR analysis. The deviations are due to either of two possibilities: severely size-dependent growth rates of the smallest nuclei, or most of the smallest nuclei are unstable, that is, less than critical size. Only a small fraction of the numbers that are counted actually grow to populate the larger sizes.

Finally, it was demonstrated that the short retention minicrystallizer, operated to vary independently seed crystal mass and size, supersaturation, and agitation rate, could be used to obtain useful design kinetics for fast growth crystallization systems. Kinetic data can be obtained from the present system with more discrimination and in a much shorter time than with conventional MSMPR techniques.

Recent studies of secondary nucleation have contributed to an understanding of the fundamental processes that determine the nucleation rate in the presence of macrosized seed crystals. Experimental approaches designed to explore the mechanisms of secondary nucleation can be roughly divided into three categories:

1. Strickland-Constable and co-workers (Lal et al., 1969, and Garabedian and Strickland-Constable 1972) and McCabe and co-workers (Clontz and McCabe, 1971, and Johnson et al., 1972) are pioneers in the study of nucleation involving single crystals. Counting and measurement of nuclei were performed by visual observation after the nuclei grew to observable size. This mode of investigation is credited for revealing the fundamental nature of contact nucleation and the importance of contact energy, area of contact, nature of contact, and surface roughness.

2. Randolph and co-workers (Randolph and Cise, 1972; Youngquist and Randolph, 1972; and Randolph and Sikdar, 1974) initiated dynamic studies of nucleation and growth in a mininucleator which was similar to MSMPR crystallizers. Use of an electronic counter made it possible to measure birth of nuclei directly, as the particles could be measured down to about 1 μm in size. Conventional sieving techniques used in the analysis of data from MSMPR crystallizers cannot discriminate mechanistic details of secondary nucleation, although such techniques are practical for determining empirical kinetic correlations. Use of the dynamic mininucleator, besides being suitable for kinetic correlations, also discriminated the mechanisms of secondary nucleation through the effects of agitation level and slurry density. The realistic crystallization environment of these experiments makes them particularly useful.

3. Larson and co-workers (Bauer, Larson, and Dallons, 1974; and Larson and Bendig, 1974) introduced a nucleator which had features of the experiments of both 1 and 2. A macrocrystal was steadily tapped in a well-stirred supersaturated medium, and the secondary nuclei were measured by a Coulter Counter. From size distribution data, the nucleation rate per crystal contact was determined. The influence of supersaturation, residence time, contact energy, and frequency of contact were studied.

Kinetic correlations of nucleation rate obtainable from experiments of types 2 and 3 are are often written in the following manner

$$B^0 = k_n(T)\ s^{k_1}\ M_k^j\ (\mathrm{RPM})^{k_2} \qquad (1)$$

The above expression has been used previously for empirical correlation of nucleation rates in MSMPR crystallizers. Bennet, Fiedelman, and Randolph (1973); Ottens and de Jong (1973); and Evans, Sarofim, and Margolis (1974) derive similar power-law expressions using a semiempirical approach. If the growth rate of crystals is size independent, the following power-law model can be used to express its dependence on supersaturation

$$G = k_g\ s^a \qquad (2)$$

Substitution of Equation (2) in Equation (1) furnishes an alternative and perhaps more frequently encountered nucleation rate expression. Thus

$$B^0 = k_n(T)\ G^i\ M_k^j\ (\mathrm{RPM})^{k_2} \qquad (3)$$

Equations (1) through (3) are useful for design purposes.

Magnesium sulfate heptahydrate is one of the most widely studied crystallization systems. However, few of these studies were carried out in a mixed suspension type crystallizer. Bauer et al. (1974) and Larson and Bendig (1974) studied nuclei generation from repetitive contacting of a macrocrystal in a continuous nucleator. These authors reported straight line log-population density vs. size plots for the magnesium sulfate system, thus indicating size-independent growth rate. Unlike magnesium sulfate, very few crystallization studies of citric acid monohydrate are reported in the literature. Moreover, meaningful nucleation or growth rate correlations are nonexistent.

The present study was undertaken along the lines of Randolph and Cise (1972) to determine the kinetics of nucleation and growth of two fast growth systems, magnesium sulfate heptahydrate and citric acid monohydrate. The primary objective was to investigate whether the mininucleator Coulter Counter assembly was adequate in determining conventional kinetics while still serving as a tool to furnish important information on mechanisms of nucleation and growth. A secondary goal was to confirm the size-independent growth rates of magnesium sulfate as reported by Bauer et al. (1974). The population balance technique was used to analyze the data.

EXPERIMENTAL APPROACH

The experimental setup used for this study was essentially the same as the one used by Cise and Randolph (1972) and described by them in detail. A carefully filtered solution of salt was pumped from a surge tank through a precooler into the well-stirred crystallizer. The 1 l crystallizer was maintained at a desired operating temperature by circulating cooling water through its jacket and an internal cooling coil. Supersaturation was achieved by cooling the crystallizer to a lower temperature than the saturation temperature of the solution in the system.

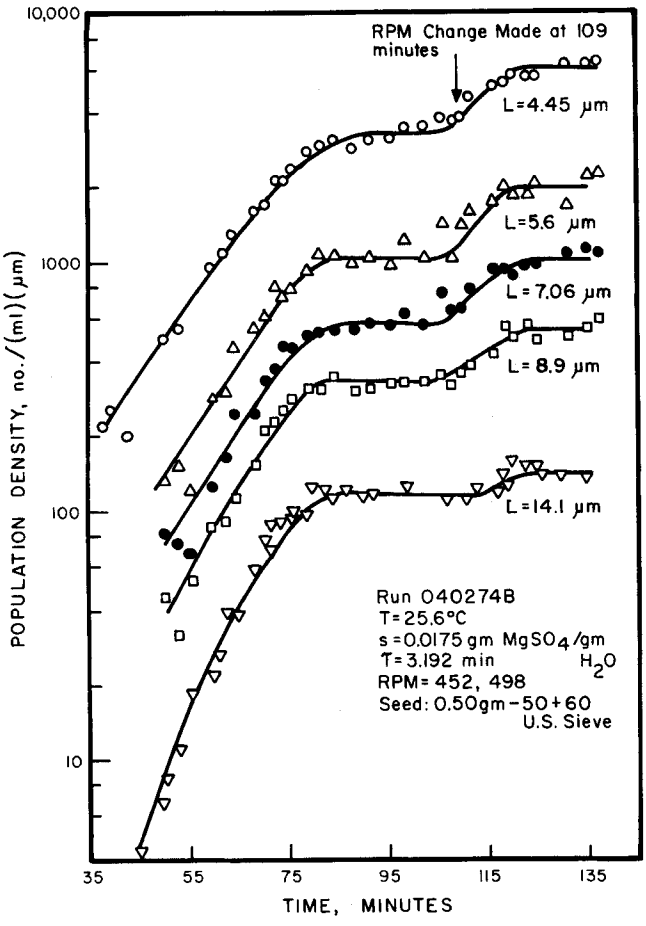

Fig. 1. Transient and quasi steady state nuclei population densities before and after a step change in stirrer RPM ($MgSO_4 \cdot 7H_2O$ system).

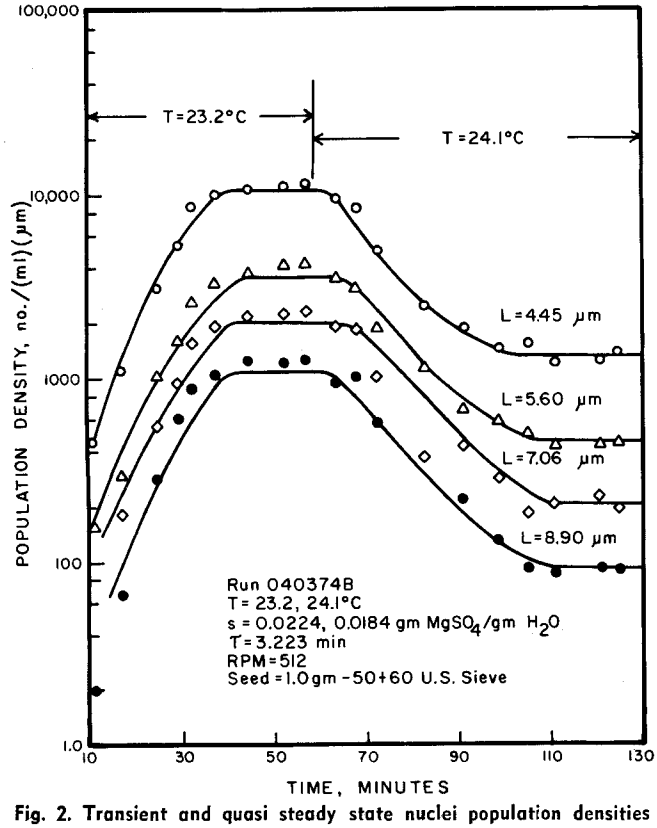

Fig. 2. Transient and quasi steady state nuclei population densities before and after a temperature change was made ($MgSO_4 \cdot 7H_2O$ system).

Microfilters were installed in the flow line to insure a clean feed to the crystallizer. Discharge from the crystallizer was through a 150 μm screen, thus permitting passage of the generated nuclei while retaining all seed crystals. This discharge was connected to the surge tank via the continuous flow sampling cell of the Coulter Counter. In this manner, direct in-situ readings of population size distribution in the crystallizer discharge were taken. The saturator described by Cise and Randolph (1972) was not packed with salt. This was done to avoid severe dust carry-over from this unit. However, owing to the very low production rate of crystals, the solution concentration in the circulating loop stayed essentially constant during a run; that is, the crystallizer acted like a differential reactor.

After a stable supersaturation level was developed in the crystallizer, the clear liquor was seeded with a small batch of commercial seeds (−50+60 U.S. standard, typically 0.25 to 1.0 g). Immediate nucleation was observed as evidenced by significant population counts in the effluent stream.

During a run, typically six to twelve samples were taken for determination of supersaturation history. Saturation concentration of magnesium sulfate heptahydrate was taken from the "International Critical Tables," Vol. 3. Solubility data of citric acid monohydrate was supplied by J. W. Mullin (University of London). Supersaturation was determined by subtracting the saturation concentration from the concentration of the mother liquor measured refractometrically. A Bausch and Lomb Type Abbe 3L refractometer was calibrated against known concentrations of solute. Density determination and the use of density vs. concentration data ("International Critical Tables," Vol. 3, p. 72, for $MgSO_4 \cdot 7H_2O$ and Kirk-Othmer "Encyclopedia of Chemical Technology," Second Edition, Vol. 5, p. 526, for citric acid monohydrate) furnished the accurate concentrations of these solutions. Any concentration could be determined by simply referring to the resulting refractive index vs. concentration calibration plot. Samples of 4.0 ml volume were taken from the crystallizer with a 5.0 ml syringe equipped with a Swinnex filter adapter. The samples were diluted by adding 4.0 ml distilled water. Refractive indexes of these diluted solutions were then determined. The concentrations of the original samples were then obtained from the concentrations of the diluted solutions by simple mass balance calculations. All concentrations were expressed as grams of anhydrous solute per gram of free water.

This study was conducted over a temperature range of 18° to 26°C and a supersaturation range of 0.0135 to 0.033 g of anhydrous solute/g of water for magnesium sulfate and a temperature range of 16° to 24°C and a supersaturation range of 0.03 to 0.13 g of anhydrous solute/g of water for citric acid. The average residence time employed was about 3 min. for the magnesium sulfate runs and 6 to 8 min. for the citric acid runs. The stirrer RPM was varied between 452 and 576. A Model *T* Coulter Counter with a 200 μm aperture tube was used to count the nuclei in the crystallizer effluent. The size range of measurement was 4.5 to 70 μm.

RESULTS

Both magnesium sulfate heptahydrate and citric acid monohydrate systems attained a quasi steady state crystal size distribution (CSD), even though the seed crystals continued to grow during a run. This situation is contrasted to the case of potassium sulfate CSD's obtained from the same experimental setup as reported by Randolph and Cise (1972) and Randolph and Sikdar (1974). Potassium sulfate fine crystal population densities for various sizes increased continuously during a run. Moreover, the CSD's on log-population density vs. size plots were extremely curved for the potassium sulfate system.

Figure 1 shows the attainment of a quasi steady state for a typical magnesium sulfate run, whereby log of population density was plotted vs. time for various sizes of fine crystals. After steady state had been achieved, a step change in the stirrer RPM was made from 452 to 498. As a result, the population density distribution assumed a new steady state level. In Figure 2 the second steady state reacts to a sudden change in the crystallizer temperature from 23.2° to 24.1°C. Figure 3 plots the corresponding

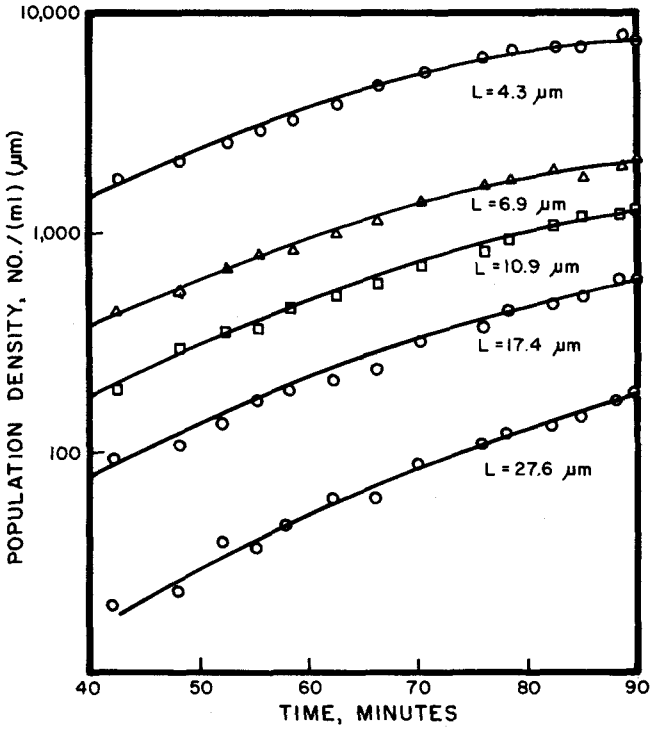

Fig. 3. Transient population densities of fine citric acid crystals (run 062774A).

transient population densities for citric acid. Fine crystal CSD's were plotted on a log-population density vs. size plots for large values of run time at which the population densities for various sizes tended to level off, thus creating a quasi steady state. Figures 4 and 5 plot such CSD's for magnesium sulfate and citric acid, respectively. Except for a few points at the lower size end of the distribution, a satisfactory linear fit was obtained. Correlation coefficients of these fits for all runs were better than 97%. However, below a size of about 8 μm a sharp deviation occurred, indicating a severely decreased growth rate or particle disappearance. Bauer et al. (1974) and Larson and Bendig (1974) reported similar observations for the magnesium sulfate system. Straight line CSD plots such as were obtained in this study are usually encountered for MSMPR crystallizers if the growth rate of crystals obeys McCabe's delta L law (size independent growth rate). The attainment of quasi steady state together with straight line CSD's on log-population density vs. size plots made it feasible to analyze the CSD data with the well-known MSMPR data reduction technique (Randolph and Larson, 1971). Data below 8 μm were not included in the analysis.

For a mixed suspension crystallizer with a constant slurry volume, clear liquor feed, negligible breakage of crystals, and birth of nuclei at a negligible size, the dynamic population balance equation takes the following form (Randolph and Larson, 1971)

$$\frac{\partial n}{\partial t} + \frac{\partial}{\partial L}(Gn) + \frac{n}{\tau} = 0 \qquad (4)$$

For size-independent growth rates at steady state, the solution of Equation (4) is the well-known MSMPR distribution:

$$n = n^0 e^{-L/G\tau} \qquad (5)$$

The slope of the steady state CSD plot is $^{-1}/G\tau$, from which growth rate of nuclei is obtainable. The effective nucleation rate B° can be defined as

$$B^0 = Gn^0 \qquad (6)$$

where n° is the intercept at L=0 on the CSD plot. In the present case of the two fast growth systems, the slowly varying transient population densities for large values of

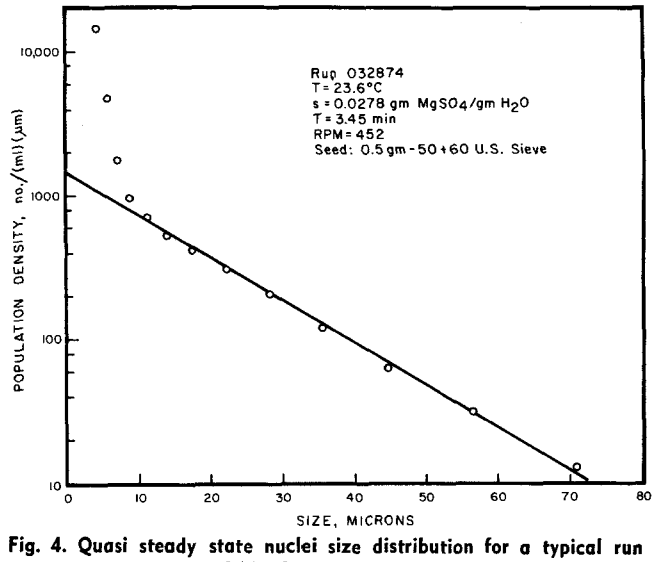

Fig. 4. Quasi steady state nuclei size distribution for a typical run of $MgSO_4 \cdot 7H_2O$ system.

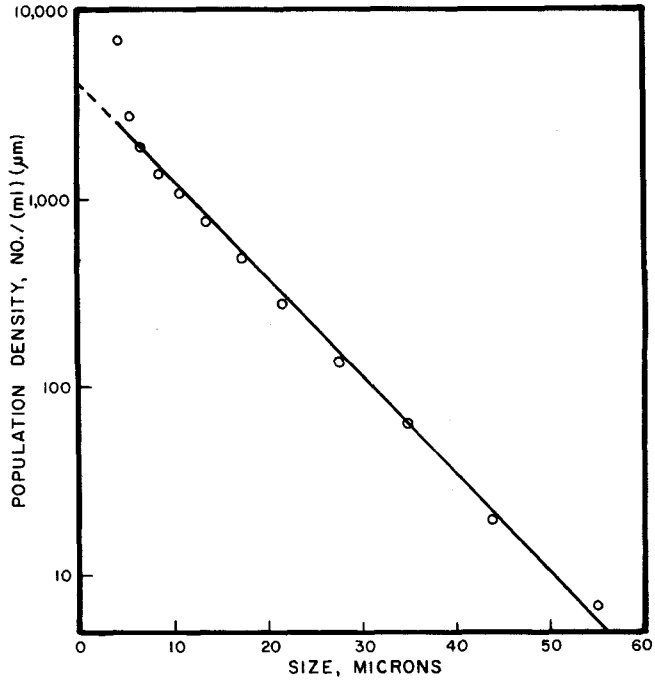

Fig. 5. Quasi steady state population density distribution of fine citric acid crystals from run 062774A at t = 82.4 min.

time together with straight line CSD's on semilog plots justify the assumption of a quasisteady state; that is, the accumulation term in Equation (4) was negligible compared to the growth and washout terms.

Growth and nucleation rates of magnesium sulfate and citric acid were obtained from the CSD plots as outlined above. Kinetic correlations of growth and nucleation rates were sought in the form of the nonlinear power-law models presented in Equations (1) and (2). For growth rates, the following kinetic correlations were obtained for the magnesium sulfate and citric acid systems, respectively:

For magnesium sulfate

$$G = \exp(8.989)s^{2.29} \quad (r^2 = 0.765) \qquad (7)$$

and for citric acid

$$G = \exp(14.28)\exp(-3\,584/T)s^{0.65} \quad (r^2 = 0.535) \qquad (8)$$

A multiple linear regression analysis library routine was used for the formulation of these correlations. Temperature was not significant at the 95% confidence level for

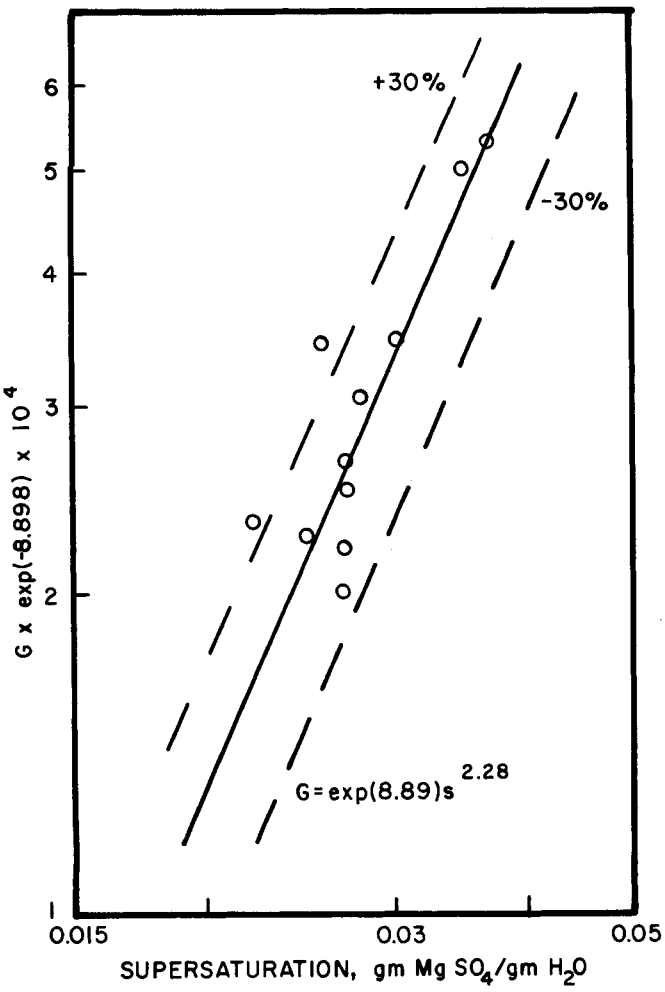

Fig. 6. Comparison between experimental and predicted growth rates of $MgSO_4 \cdot 7H_2O$.

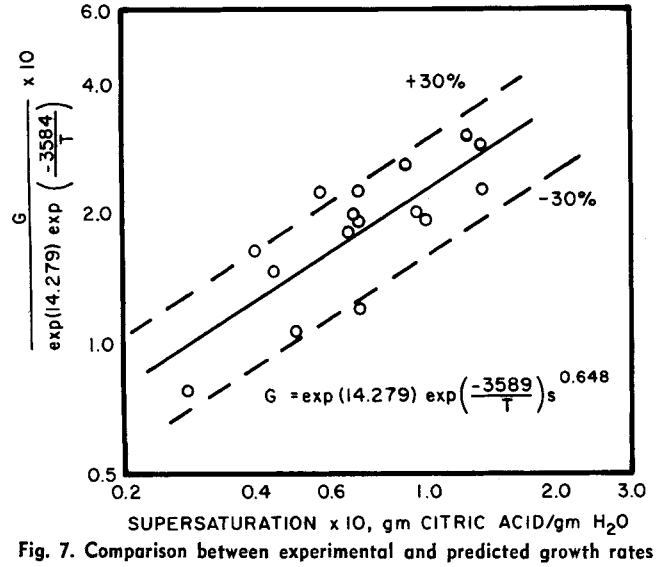

Fig. 7. Comparison between experimental and predicted growth rates of citric acid.

magnesium sulfate. Agitator RPM was found to have no effect on the growth rates. Absence of an RPM dependency indicates that the fine crystal growth rates represented by Equations (7) and (8) are independent of bulk diffusional effects at the levels of agitation considered in this study. Supersaturation dependencies of the growth rates of magnesium sulfate and citric acid are shown in Figures 6 and 7, respectively. Thirty percent deviations from the predicted line are marked by dotted lines.

Nucleation rates of magnesium sulfate and citric acid correlated with supersaturation, temperature, and slurry properties. The following kinetic relationships were obtained:

For magnesium sulfate

$$B^0 = \exp(-51.96)\, s^{2.59} \exp(21\,346/T)\, M_T^{0.67} \qquad (r^2 = 0.757) \quad (9)$$

and for citric acid

$$B^0 = \exp(-8.735)\, s^{0.543} \exp(4\,781/T)\, M_4^{0.84} \qquad (r^2 = 0.63) \quad (10)$$

Agitator RPM did not effect B° for either system. The third moment of the seed crystal distribution (represented by the solids concentration M_T) furnished the best correlation of magnesium sulfate nucleation rate. For citric acid, Equation (10) involving the fourth moment appeared to be the best correlation. Figures 8 and 9 show the correspondence between the observed nucleation rates of these two systems and those predicted by the power-law correlations of Equations (9) and (10).

Both growth and nucleation rates of magnesium sulfate show strong dependence on supersaturation [Equations (7) and (9)] in contrast to low-order dependencies for citric acid. The importance of the term represented by the moments of the parent macrocrystals indicates secondary breeding. Such a dependence would be expected from the single crystal studies mentioned earlier. Since collision energy and collision frequency are known to be primary variables determining secondary nucleation, one would expect the agitation level (RPM) to affect the nucleation rates of the two systems studied. A large effect of stirrer RPM is observed at the smaller sizes (Figure 1). The population densities of the larger sizes, which were extrapolated to determine the nucleation rate, did not show a marked effect due to RPM. Thus, the significant RPM dependence observed at the smaller sizes never shows up as perturbations in the larger size ranges. A similar observation was made with the citric acid system. Possible explanations of this apparent discrepancy are given in the next section.

Table 1 compares the kinetic dependencies of the nucleation rates found in this study with those published in the literature. Ranges of observed growth and nucleation rates were 1.54 to 4.23 μm/min. and 2 382 to 9 673 No./(cm^3) (min.) for magnesium sulfate and 0.66 to 2.21 μm/min. and 650 to 5 164 No./(cm^3) (min.) for citric acid, depending on conditions. Listed in Table 2 are values of observed growth and nucleation rates at a median supersaturation and RPM.

DISCUSSION

Three significant observations in the small size range (<8 μm) were made during these experiments.

1. Small particles below 8 μm exhibit significantly higher population densities than expected by semilog extrapolation from the larger sizes.

2. Particle counts in this small size range decreased significantly with a decrease in supersaturation.

3. Agitation level (stirrer RPM) effected this size range much more significantly than the larger sizes.

The second item suggests that the particles were real. The significant curvature in the population density plot (item 1) would then be attributed either to a grossly lower particle growth rate below 8 μm or nonsurvivability of such nuclei. Such a dramatic decrease in growth rate is not readily explained by current growth rate theories. However, Strickland-Constable et al. theorize

Table 1. Dependencies of Nucleation Rates on Operating Variables

	Supersaturation	M_j	RPM
$MgSO_4 \cdot 7H_2O$*	$s^{2.59}$	$M_T^{0.67}$	Insignificant
$MgSO_4 \cdot 7H_2O$†	$s^{2.7}$	—	$RPM^{4.5}$
$MgSO_4 \cdot 7H_2O$**	$s^{3.0}$	—	—
$MgSO_4 \cdot 7H_2O$††	$s^{4.0}$	—	—
Citric acid monohydrate*	$s^{0.543}$	$M_4^{0.84}$	Insignificant

* From this tudy.
† From Ness and White (1974).
** From Larson and Bendig (1974).
†† From Bransom et al. (1969).

that slow growth of nuclei could be attributed to their initial degree of perfection.

Resistance to bulk diffusion of solute in solution can cause size-dependent growth rates. Rosen (174) showed that in multiparticle stirred suspensions, slip velocity increases with particle size. The work of McCabe and Stevens (1951), Mullin and Gaska (1969), and Rosen and Hulburt (1971), among others, demonstrated that the growth rate of a single crystal increases with increasing slip velocity and finally asymptotes to a constant growth rate when the resistance to mass transfer due to diffusion is eliminated. This asymptotic growth rate corresponds to the particle integration step controlling the process of growth. However, the insensitivity to RPM of nuclei growth rates obtained in this study indicates that diffusion was not a factor at such small sizes. This is consistent with the boundary-layer theories of diffusion resistance. Further, diffusion-caused size-dependence in growth rate would be more gradual and would occur over a larger size range than the abrupt change in population density data observed at about 8 μm.

The question may be asked if the counts given by the Coulter Counter are correct in this small size range. Both items 2 and 3 seem to indicate that the particles actually exist at the conditions measured. Extensive mass and number balance experiments with 50, 100, and 200 μm aperture tubes with 3.5, 5.7, and 19 to 20 μm light calibration particles and 5 to 10 μm glass beads demonstrated that the Counter gave reliably accurate counts except for the three smallest sizes (4.4 to 7.0 μm) in the span of 200 μm aperture tube. However, a knowledge of the estimate of the spurious counts obtained from the calibration experiments could not be reliably used to correct for the high counts obtained below 8 μm for the crystallization experiments of this study (Sikdar, 1975). Item 3 could best be explained if the particles below 8 μm were unstable, with few surviving to populate the larger size ranges. These particles are directly observed in the present short retention experiments but might never be measured in conventional long retention MSMPR experiments. Disappearance of the unstable nuclei would explain why the large RPM dependence observed for sizes <8 μm never resulted in a marked agitation dependence (RPM was not significant at the 95% confidence level) in the nucleation correlation obtained by extrapolation from the larger particle sizes. In another study, Randolph and Sikdar (1975) experimentally demonstrated that a large majority of initially formed potassium sulfate nuclei (which can be counted) never survive to populate the large sizes. Similarly, in the present case with the magnesium sulfate and citric acid systems, it is possible to attribute the deviations from straight line CSD's on semilog plots at sizes <8 μm to the instability of these nuclei. It is difficult to conceive of the dramatic decreases in growth rate, as envisaged in the theory of crystal perfection of Garabedian and Strickland-

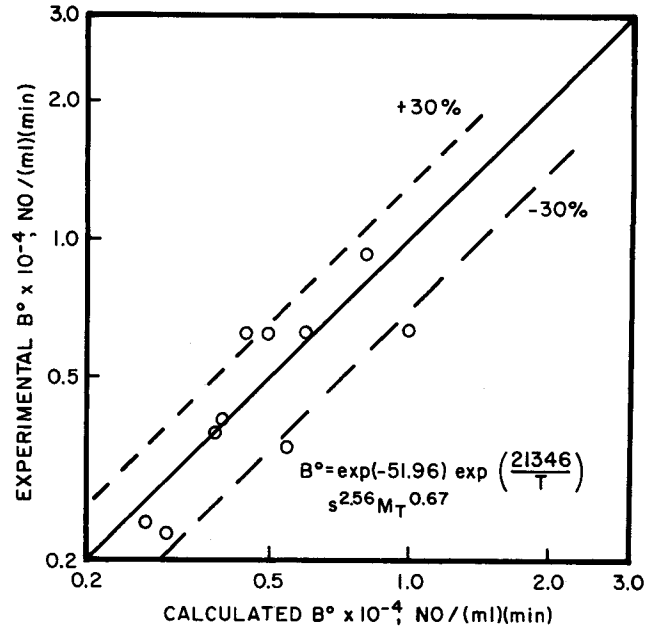

Fig. 8. Comparison between experimental and calculated nucleation rates of magnesium sulfate.

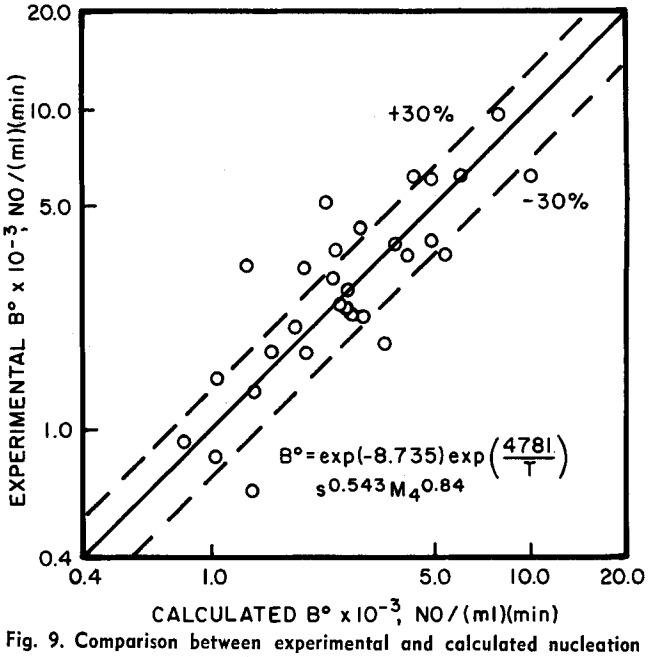

Fig. 9. Comparison between experimental and calculated nucleation rates of citric acid monohydrate.

Table 2. Growth and Nucleation Rates at a Median Supersaturation and RPM

	T, min.	g solute/g H_2O	RPM	G, μm/min.	B°, No./(cm³)(min.)	M_T, g/cm³	Time, min
$MgSO_4 \cdot 7H_2O$ system run 040174	3.33	0.027	498	2.12	3 976	0.052	71.5
Citric acid system run 062574A	7.26	0.069	536	1.39	3 518	0.012	50.0

Constable (1972), which would explain the anomalous population densities below 8 μm.

Growth rates for magnesium sulfate crystals obtained in this study verified Bauer et al.'s observation of the size independence of growth rates, at least for sizes <8 μm. However, the supersaturation dependence of growth rate of $s^{2.24}$ for magnesium sulfate obtained in this study is at variance with $s^{1.4}$ obtained by Larson and Bendig (1974) and $s^{1.0}$ reported by Bransom and Brown (1969). Data from all these studies were taken from continuous-flow stirred-tank crystallizers. The RPM independence of growth rate for both magnesium sulfate and citric acid, together with a supersaturation dependence substantially different from unity (as expected for diffusion controlled growth), indicates that growth rate is controlled by particle integration in the crystal lattice.

Kinetic correlation of nucleation rate for magnesium sulfate heptahydrate [Equation (9)] compared to that for citric acid [Equation (10)] illustrates the higher dependence of magnesium sulfate nucleation on supersaturation ($s^{2.59}$) as well as temperature. While B° of magnesium sulfate heptahydrate correlated with M_T, a much better correlation was obtained with M_4 for citric acid monohydrate. The effect of the impeller RPM on the nucleation rates for both systems was found negligible. Besides particle instability, another possible explanation exists for the absence of an RPM function in the nucleation correlation. Thus, at the level of agitation nucleation is surface regeneration limited implying stress saturation at the surface of the seed crystals. Sung et al. (1974) noted that this was the case in the nucleation of magnesium sulfate caused by an impinging fluid jet on a single crystal. A mechanism of nucleation has been suggested by Wang and Estrin (1974) which appears to explain the magnesium sulfate heptahydrate nucleation correlation obtained in this study. These authors formulated a growth limited nucleation model according to which surface irregularities (dendrites) of the seed crystals are broken off as nuclei in the supersaturated solution. The growth or regeneration of these surface irregularities can limit the nucleation rate if adequate mechanical stimulation is present for removal from the surface. From the second-order supersaturation dependence of the growth of the dendrites and the first-order variation of the number of sites, a third-order nucleation rate is predicted. The $s^{2.59}$ dependence of B° obtained in this study may be considered to be in fair agreement with the predicted behavior. B° is predicted independent of impeller RPM (as found in this study), since collision frequency does not limit the formation of nuclei. The observed proportionality between B° and M_T would also be expected because the number of dendritic sites depends on the amount of crystals present in suspension. The growth limited nucleation proposed by Wang and Estrin is in direct contrast to removal limited nucleation model proposed by Evans et al. (1974). The latter formulation predicts B° to be strongly influenced by the agitation level as found in the study of potassium sulfate (Randolph and Sikdar, 1975). Citric acid monohydrate nucleation rates also were found to be independent of impeller RPM; however, the supersaturation dependence cannot be explained by the Wang-Estrin model. In contrast to second-order growth and third-order nucleation, both growth and nucleation rates were found to be proportional to approximately the square root of supersaturation. It is of interest to note that the nucleation sensitivity parameter i of Equation (3) was found to be reasonably close to unity for both magnesium sulfate and citric acid systems (1.12 and 0.83, respectively). This leads to the speculation (at least for fast growth systems) that nucleation and growth phenomena may be intimately related (McCabe and Rousseau, 1974).

ACKNOWLEDGMENT

The authors acknowledge the financial support provided by National Science Foundation through Grant No. GK-36517X. The magnesium sulfate part of this work was presented at the 77th National AIChE meetings at Pittsburgh, Pennsylvania, in June, 1974.

NOTATION

B^0 = nucleation rate, No./(cm^3) (min.)
G = linear growth rate, μm/m
i = kinetic power on growth rate in nucleation rate correlation
j = kinetic power on solids concentration in nucleation rate correlation
k_g = growth rate kinetic constant
k_n = nucleation rate kinetic constant
L = linear size, μm
M_T = solids concentration g/cm^3
M_k = k^{th} moment of macrocrystals
n = population density, No./(cm^3) (μm)
n^0 = steady state nuclei population density
r^2 = linear correlation coefficient
s = supersaturation; g anhydrous solute/g of water
T = absolute temperature, K
τ = average residence time, m

LITERATURE CITED

Bauer, L. G., M. A. Larson, and V. J. Dallons, "Contact Nucleation of $MgSO_4 \cdot 7H_2O$ in a Continuous MSMPR Crystallizer," *Chem. Eng. Sci.*, **29**, 1253 (1974).

Bennett, R. C., H. Fiedelman, and A. D. Randolph, "Crystallizer Influenced Nucleation," *Chem. Eng. Progr.*, **69** No. 7, 86 (1973).

Bransom, S. H. and D. E. Brown, Presented at Symp. on Ind. Crystallization, London, England (April, 1969).

Cise, M. D., and A. D. Randolph, "Secondary Nucleation of Potassium Sulfate in a Continuous-Flow, Seeded Crystallizer," *AIChE Symp. Ser. No. 121*, **68**, 42 (1972).

Clontz, N. A., and W. L. McCabe, "Contact Nucleation of Magnesium Sulfate Heptahydrate," *Chem. Engr. Progr. Symp. Ser. No. 110*, **67**, 6 (1971).

Evans, T. W., A. F. Sarofim, and G. Margolis, "Models of Secondary Nucleation Attributable to Crystal-Crystallizer and Crystal-Crystal Collisions," AIChE J. *20* No. 5, 959 (1974)

Garabedian, H., and R. F. Strickland-Constable, "Collision Breeding of Crystal Nuclei: Sodium Chlorate II," *J. Crystal Growth*, **12**, 53 (1972).

Johnson, R. T., R. W. Rousseau, and W. L. McCabe, "Factors Affecting Contract Nucleation," *AIChE Symp. Ser. No. 121*, **68**, 31 (1972).

Lal, D. P., R. E. A. Mason, and R. F. Strickland-Constable, "Collision Breeding of Crystal Nuclei," *J. Crystal Growth*, **5**, 1 (1969).

Larson, M. A., and L. L. Bendig, "Nuclei Generation From Repetitive Contacting," *ERI-74152*, Iowa State Univ., Ames (1974).

McCabe, W. L. and R. W. Rousseau, GVC/AIChE Joint Meeting, Munich, Preprints Vol. 1, p.A5-1 (1974).

McCabe, W. L., and R. P. Stevens, "Rate of Growth of Crystals in Aqueous Solutions," *Chem. Eng. Progr.*, **7**, No. 4, 168 (1951).

Mullin, J. W., and C. Gaska, "The Growth and Dissolution of Potassium Sulfate in a Fluidized Bed Crystallizer," *Can. J. Chem. Eng.*, **47**, 483 (1969).

Ness, J. N., and E. T. White, "Collision Nucleation in an Agitated Crystallizer," Paper presented at 77th National AIChE meeting, Pittsburgh, Pa. (1974).

Ottens, E. P. K., and E. J. de Jong, "A Model for Secondary Nucleation in a Stirred Vessel Cooling Crystallizer," *Ind. Eng. Chem. Fundamentals*, **12**, 179 (1973).

Randolph, A. D., and M. D. Cise, "Nucleation Kinetics of the Potassium Sulfate-Water System," *AIChE J.*, **18**, No. 4, 806 (1972).

Randolph, A. D., and M. A. Larson, *Theory of Particulate*

Processes, Academic Press, New York (1971).
Randolph, A. D., and S. K. Sikdar, "Effect of a Soft Impeller Coating on the Net Formation of Secondary Nuclei," *AIChE J.*, **20**, No. 2, 410 (1974).
———, "Survival of Secondary Crystal Nuclei of K_2SO_4," Preprints Vol. 1, p.A5-3, GVC/AIChE Joint Meeting, Munich (1974).
Randolph, A. D., and S. K. Sikdar, "Creation and Survival of Secondary Nuclei: The K_2SO_4-Water System," in press (1975).
Rosen, H. M., "Importance of Slip Velocity in Determining Growth and Nucleation Kinetics in Continuous Crystallization," *AIChE J.*, **20**, No. 2, 388 (1974).
———, and H. M. Hulburt, "Continuous Vacuum Crystallization of Potassium Sulfate," *Chem. Eng. Progr. Symp. Ser. No. 11*, **67**, 18 (1971).
Sikdar, S. K., "Secondary Nucleation Mechanisms and Kinetics in a Continuous-Flow, Seeded Crystallizer," Ph.D. dissertation, Univ. Ariz., Tucson (1975).
Sung, C. Y., G. R. Youngquist, and J. Estrin, "Secondary Nucleation by Fluid Shear," Preprints Vol. 1., p.A5-2, GVC/AIChE Joint Meeting, Munich (1974).
Wang, M. L., and J. Estrin, Dept. of Chemical Engineering, Clarkson College of Technology, Potsdam, New York, Private Communication (1974).
Youngquist, G. R., and A. D. Randolph, "Secondary Nucleation in a Class II System: Ammonium Sulfate-Water," *AIChE J.*, 18, 421 (1972).

Manuscript received May 9, 1975; revision received September 3 and accepted September 4, 1975.

Solubility of Gases and Liquids in Molten Polystyrene

Experimental solubility data have been obtained for sixteen organic solutes in molten polystyrene by a gas chromatographic procedure for temperatures from 408° to 503°K and pressures to 4 atm. The effects of diffusion and adsorption of the solute on the substrate were considered. The Henry's law constants resulting from this study and those obtained by other investigators were related to the reduced temperature. The effect of pressure on the Henry's law constants is also discussed, and a relationship is presented for the heat of solution.

LEONARD I. STIEL
and
DANIEL F. HARNISH

Allied Chemical Corporation
Specialty Chemicals Division
Buffalo, New York

SCOPE

Solubility values of gases and liquids in molten polystyrene are required in several important applications. For example, in the extrusion process for the production of polystyrene foam, an expansion agent is injected into the polymer at an elevated temperature and pressure and subsequently released at a lower temperature and pressure. An important physical variable influencing the quality and cost of the foam is the solubility of the agent at the initial and final stages of extrusion.

For molten polystyrene, solubility data have previously been reported for gases at elevated pressures and for liquids at low pressures. An examination of the solubilities from the various sources revealed some inconsistencies, and a need was established for additional data, particularly for substances with values intermediate to those of R-22 and *n*-pentane. Therefore, in the present study, solubility measurements have been obtained for sixteen organic solutes, and the available data have been utilized to develop a generalized method for the calculation of this property.

CONCLUSIONS AND SIGNIFICANCE

For amorphous polyethylene, Stern et al. (1969) found that the available solubility data could be represented by a linear relationship between the log of the Henry's law constant and $(T_c/T)^2$. In this study, a similar approach has been found to be applicable for the solubility of gases and liquids in molten polystyrene. The Henry's law constants obtained from various sources have to be initially reduced to a common basis.

The Henry's law constants presented in this study enable the estimation of solubilities for a number of substances for which data were previously not available. The correlation of the available data enables the calculation of solubilities for additional substances. The effect of pressure on the solubilities can be estimated by use of the relationships discussed.

The chromatographic method is a useful procedure for the determination of solubilities in polymers. The correlation of the data aids in the analysis of the measurements.

For molten polystyrene, the available solubility data include the values of Newitt and Weale (1948) for hydrogen, nitrogen, carbon dioxide, and ethylene for 403° to 463°K and 80 to 300 atm.; Lundberg et al. (1962, 1963) for methane for 373° to 461°K and 80 to 325 atm.; and Durrill and Griskey (1966) for nitrogen, carbon dioxide, helium, argon, and chlorodifluoromethane (R-22) at 462°K and pressures to 20 atm. These investigators utilized high pressure sorption experiments in which solubility and diffusivity data were simultaneously obtained. Duda and Vrentas (1968) obtained solubilities and diffusivities for *n*-pentane at 1 atm and 413° to 443°K by the use of a quartz spring sorption apparatus. Similar measurements were made by Duda et al. (1973) for ethylbenzene for